Constructing the transition graphs of interacting hysterons

Margot Teunisse and Martin van Hecke
Universiteit Leiden
(Dated: June 28, 2022)

Structure:

I. INTRODUCTION

Frustrated media can have rugged energy landscapes, with many metastable states. Recent work has shown that the many metastable states in frustrated systems can lead to unusual pathways when the system is subject to driving. For a variety of systems, including sheared amorphous solids[1][2], crumpled thin sheets[3], corrugated sheets[4] and origami structures[5] remarkable phenomena such as breaking of return-point memory, a multiperiodic response to cyclical driving, and transient memory as described by the park bench model [1][6] have been observed.

It turns out that the response of many frustrated systems can be captured by an interacting collection of hysteretic two-state elements, called hysterons. The hysteron model, first suggested by Ferenc Preisach[7], has long been used to model hysteretic systems as a collection of small hysteretic two-state elements. However, the Preisach model considers hysterons to be independent, while the interacting hysteron model has remained largely unexplored. The recent experimental findings show that the interacting hysteron model is relevant for many physical systems, and thus worth examining in more detail.

The possible metastable states and transitions between these states for a given hysteron system can be portrayed as a directed graph, which captures all possible responses of the system to driving[8]. Numerical sampling work from our group has shown that the number of possible transition graphs for a system of interacting hysterons increases dramatically with the number of hysterons. For as few as three interacting hysterons, over 15,000 distinct graphs are found[9]. Because the number of possible transition graphs quickly grows overwhelming, a systematic method will be needed for categorizing the graphs.

Here we establish a systematic method to gradually approach the complexity of the interacting hysteron model, starting from the Preisach model. We first establish a formalism for constructing the transition graph for coupled hysterons by starting from a Preisach graph, and adding the effects of coupling step-by-step. We show how this formalism is used to construct a list of candidate graphs for a given number of hysterons. We then detail a method for checking whether a given transition graph can be realized, both in general and for a specific model. Finally, we illustrate our formalism for a model where hysterons are linearly coupled.

II. MODEL

Here we detail the basic setup for simulating a system of N hysterons. We define the state of the system S as

$$S = \{s_1, s_2, ..., s_N\} \tag{1}$$

where $s_i \in \{0, 1\}$ are the phases of individual hysterons. We then model the response of individual hysterons to an external driving field U by defining up and down switching fields U_i^+ and U_i^-. A hysteron transitions from phase 0 to 1 ('up') if $U \geq U_i^+$, and from phase 1 to 0 ('down') if $U \leq U_i^-$.

If the system of hysterons is non-interacting, then the switching fields $\{U_i^+\}, \{U_i^-\}$ are fixed values $u_i^{+,-}$. We refer to these switching fields in the absence of interactions as the bare switching fields. If there are interactions, the switching fields are modified by the state S:

$$U_i^{+,-}(S) = u_i^{+,-} + \Delta u_i(S) \tag{2}$$

When a driving field U is applied to a system with the collective state S, any hysterons that are in phase 0 and have $U \geq U_i^+$, or that are in phase 1 and have $U \leq U_i^-$, become unstable. If a single hysteron is unstable, that hysteron flips. If multiple hysterons are unstable, the system's response is ambiguous, as it is unclear which hysteron flips first and these operations do not commute if there is coupling. We therefore do not consider cases where multiple hysterons are unstable.

It can occur that the flipping of one hysteron destabilizes other hysterons when there is coupling. It may therefore take multiple iterations for the system to reach stability under a field U. We refer to this phenomenon as an avalanche. It is also possible that an avalanche leads back into the state itself, in which case the system becomes caught in a self-loop. We consider this scenario to be ill-defined, as the system's state is caught in an infinite loop.

The system's response to a field U is thus obtained by comparing the field to the switching fields $\{U_i^+\}, \{U_i^-\}$ of the hysterons individually, flipping hysterons that are unstable, and repeating this process until there are no more unstable hysterons. The response is ill-defined if multiple hysterons are unstable at the same time, or if the system becomes caught in an infinite self-loop.

The possible responses of a collection of N hysterons to driving are captured by a state transition graph, which consists of all stable states S and all transitions between states. For a system of N hysterons, there are 2^N possible states. In particular there are two saturated states,

where either all $s_i = 0$ or all $s_i = 1$. Each state S has a single up and down transition, except for the two saturated states, which only have an up and a down transition respectively. Therefore, a transition graph for a collection of N hysterons consists of a maximum of 2^N states and $2(2^N - 1)$ transitions. It can occur that not all of the 2^N states are included in the transition graph, because it is possible for a state to not be reachable, or to only be reachable as an unstable intermediate state of an avalanche. We discuss unreachable states in more detail in Section III A.

A. Evaluation of switching fields

We now describe how the transition graph is constructed for a given set of bare switching fields $\{u_i^{+,-}\}$ and coupling coefficients c_{ij}.

We observe that in essence, it is only the ordering of the switching fields $U_i^{+,-}(S)$ that determines the state transition graph, rather than their absolute value. As a result, there can only be as many graphs as there are permutations of the order of switching fields. In the case where hysterons are non-interacting, there are only $2N$ switching fields $\{u_i^{+,-}\}$. In addition, because we never compare an up switching field with a down switching fields, the only orderings that can change the graph are the partial orderings of the up switching fields $\{u_i^{+}\}$ and of the down switching fields $\{u_i^{-}\}$. The number of orderings that can lead to a unique graph is then $N! \times N!$. When we fix the up switching fields to account for exchange symmetry, we find that the number of permutations is only $N!$. Indeed, we have that there are $N!$ Preisach graphs for a collection of N hysterons, each corresponding to a different main loop.

When hysterons are allowed to interact, however, the situation changes. On one hand, there are then $2(2^N - 1)$ states $U_i^{+,-}(S)$, and because of the possibility of avalanches, the ordering between all of the states must be considered. On the other hand, the state transition graph is only determined by a partial order between some of the switching fields. As a result, the number of permutations greatly outnumbers the number of unique state transition graphs. For $N = 2$, the number of permutations is $8! = 40320$ while we know the number of graphs to be 13. For $N = 3$, the number of permutations is as high as $24! \approx 6 \times 10^{23}$.

We conclude that it is inefficient to find all graphs for an interacting system of hysterons by considering the permutations of all switching fields. Even so, we can make use of the fact that the state transition graph only depends on a partial ordering of the switching fields. Namely, we know that each graph has an underlying set of linear inequalities $U_i(S_A) > U_j(S_B)$, which we refer to as the design inequalities[9]. The solution space of the design inequalities provides the region in parameter space that leads to the given graph. In particular, if the design inequalities have no solution, then the given graph is not realizable.

III. CONSTRUCTING POSSIBLE GRAPHS

In recent work, the transition graphs for two- and three-hysteron systems were found using numerical sampling. The obtained graphs contain several noteworthy phenomena that are not possible in the Preisach model, such as breaking of loop return point memory, scrambling, multiperiodic cycles and long transients[9].

A significant disadvantage of numerical sampling is that it is not conclusive, as it is always possible that a region in parameter space leading to a certain transition graph is missed. Here we aim to establish a tool that can conclusively find all possible graphs for a given number of hysterons N.

Fortunately, it is not necessary to sample all of parameter space. The reason for this is that the transition graph for a given system does not depend on the absolute values of the switching fields $U_i^{+,-}(S)$, but only on the order of the switching fields. In principle, one could find all possible transition graphs for a given number of hysterons N by evaluating all permutations of the order of the switching fields.

In practice, however, it is impractical to find the possible transition graphs by evaluating all possible orderings. This is because the transition graph only depends on a partial order of the switching fields, not on the total order, so that the number of permutations vastly outweighs the number of possible graphs. For example, for the interacting two-hysteron system, there are eight switching fields, giving $8! = 40320$ permutations, and for $N = 3$ the number of permutations is $24! \approx 6 \times 10^{23}$.

Instead of evaluating all permutations of the total order of the switching fields, we find it more useful to take a reverse approach by starting from the topology. We first construct a number of candidate graphs, which describe the behaviour of a hysteron system in a well-defined way but are not necessarily realizable. We then check whether each graph is realizable by evaluating whether there is a region in the parameter space of switching fields corresponding to the graph.

The region in parameter space associated with each graph is bounded by a set of linear inequalities that the switching fields must obey, which we refer to as the design inequalities. We generate the design inequalities systematically by combining the conditions on each individual transition. We describe how the design inequalities are found in the Supplemental Information. If the solution space of a graph's design inequalities is not empty, then the graph is realizable. Thus, one can find the possible graphs for N hysterons by first generating the candidate graphs, then checking whether each graph's design inequalities have a solution.

In addition to being an efficient method for conclusively finding the possible graphs, the method of can-

didate graphs also allows us to consider rational design of graphs. We can use the candidate graph method to directly consider the possibility of the interesting behaviours that have been observed previously, such as multiperiodic cycles and long transients, for a given number of hysterons.

We here establish our method for finding the transition graphs that are possible for coupled hysterons. We first discuss in section III A how one can generate a list of candidate graphs that includes all possible graphs for a given number of hysterons N. Next, in section III B, we explain how to evaluate whether or not a graph is realizable by checking whether its underlying design inequalities have a solution. Finally, we improve on the candidate graph method by introducing the concept of base graphs.

A. Candidate graphs

A well-defined transition graph for N hysterons consists out of 2^N states, and $2(2^N-1)$ transitions, namely the up and down transitions from each state, except for the saturated states which only have one transition each. A transition graph is constructed by choosing a transition path for each of these $2(2^N-1)$ transitions. A transition path may be a single hysteron flip, or may consist of multiple flipped hysterons. When a transition path consists of multiple hysteron flips, we speak of an avalanche.

Naively, one can construct all possible transition graphs by finding the possible transition paths for each individual transition. For example, for $N = 2$ one finds $3^4 \times 6^2 = 2916$ graphs (Fig.1). We will now make two considerations that reduce the number of candidate graphs, namely exchange symmetry and garden-of-Eden states.

1. *Exchange symmetry*

The hysterons in our model are considered as indistinguishable particles. That is, when we define the state $S = \{s_1, s_2, ..., s_N\}$, the labelling of hysterons 1 through N is arbitrary. As a result, when two graphs only differ from one another by the ordering of the hysterons 1, 2, ..., N, we consider the graphs to be the same (Fig. 2a).

To account for exchange symmetry, we fix the order in which hysterons 1, 2, ..., N flip up when increasing the external field from the ground state. For example, for $N = 3$, we have that hysteron 3 flips up first from the state 000, hysteron 2 flips up first from 001, and trivially hysteron 1 flips up first from 011. Since there are $N!$ permutations of the order of N hysterons, accounting for exchange symmetry decreases the number of candidate graphs by a factor $N!$. Thus, for $N = 2$, the number of candidate graphs is reduced by a factor 2 from 2916 to 1458.

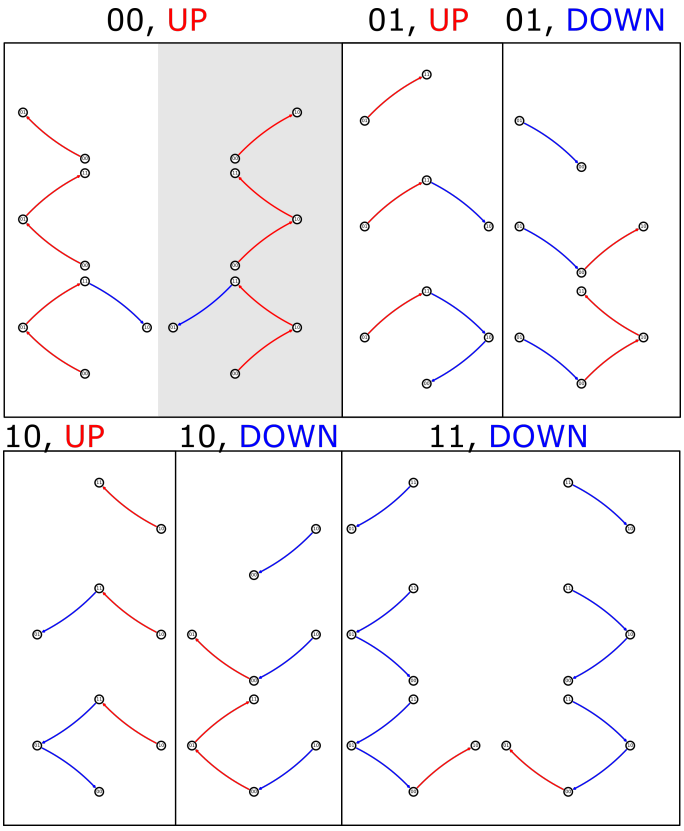

FIG. 1. Overview of the possible transition paths for each $N = 2$ transition individually. The greyed-out area signifies transitions that are left out when accounting for exchange symmetry.

2. *Garden-of-Eden states*

It often occurs that one or more of the possible states for N hysterons cannot be reached from the ground state. As is customary[5], we refer to states that cannot be reached as garden-of-Eden (GoE) states. We may choose to exclude GoE states in some cases, for instance in an experimental setup where one starts from the ground state. As a consequence of excluding GoE states, when two graphs only differ from one another by transitions that occur from GoE states, the graphs become duplicates. Therefore, when GoE states are ignored, the number of distinct graphs can turn out lower than the number of possible combinations of transitions. For $N = 2$, ignoring GoE states reduces the number of graphs from 1458 to 752.

B. Realizability

To better understand why some graphs are not realizable, we look in detail at the design inequalities underlying the graphs (see SI), and identify the inequalities that are in conflict with one another. By then

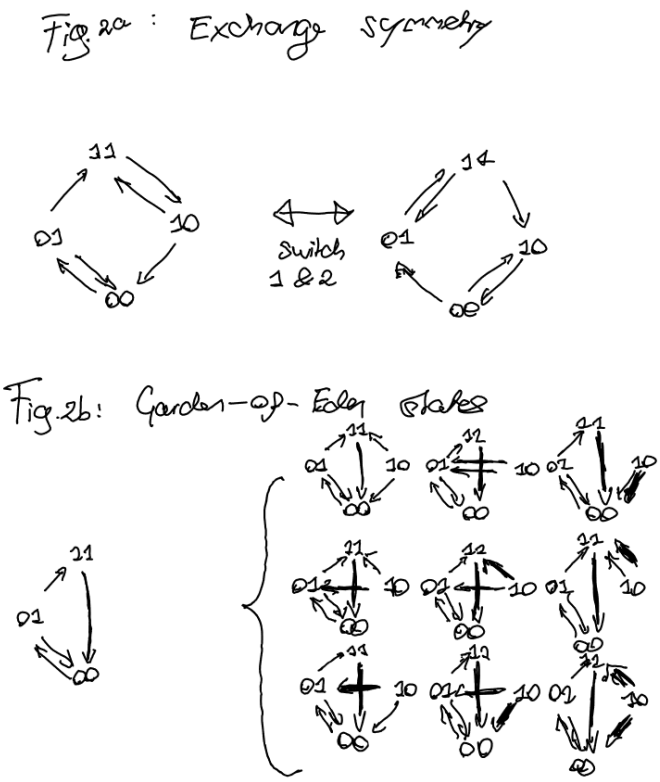

FIG. 2. Considerations for removing duplicate graphs: a) exchange symmetry and b) garden-of-Eden states.

tracing these inequalities back to the transitions from which we arise, we find the combinations of transitions (i.e., subgraphs) that are incompatible and thus make a graph not realizable. Several examples of impossible subgraphs are given in Fig. 3a.

We now direct our attention to a particular group of impossible subgraphs, an example of which is shown in Fig. 3b. The example subgraph consists of the single-flip transition $11 \downarrow 10$, and the avalanche $10 \uparrow 11 \downarrow 01$. We observe that the transition $11 \downarrow 10$ requires that $U_2^-(11) > U_1^-(11)$ to have hysteron 2 flip down from the state 11. Conversely, the transition $10 \uparrow 11 \downarrow 01$ requires the inequality $U_1^-(11) > U_2^-(11)$ to have an avalanche where only hysteron 1 flips down from the state 11. The contradiction between the two transitions arises because the avalanche $10 \uparrow 11 \downarrow 01$ imposes that the switching field U_1^- is the highest down switching field, even though the transition $11 \downarrow 01$ is only a part of a larger avalanche. The argument used for the example subgraph can be extended to the general argument that the up and down flips which can occur from a state do not depend on whether or not that state is stable. As a consequence, all avalanches occuring in a graph must conform to an underlying graph of single-flip transitions, which we refer to as the base graph.

Using base graphs, we can improve upon our method for generating candidate graphs. Namely, by first constructing all base graphs, and only then evaluating

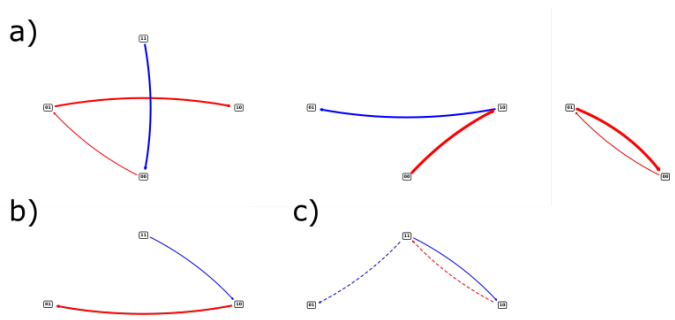

FIG. 3. Examples of impossible combinations of transitions for the two-hysteron system. a) Several examples of impossible combinations of transitions. b) Example of an combination of transitions that is impossible due to a violation of the underlying base graph. c) Illustration of how the combination of transitions in (b) violates the underlying base graph.

all possible avalanches for each base graph individually, we exclude the subgraphs of the type shown in Fig. 3b from the outset. Because the number of graphs for which the design inequalities need to be explicitly generated is then reduced, the base graph method has an improved efficiency compared to the naive approach.

In addition to the base graph method being an efficient method for generating candidate graphs, it also providedes us with a powerful framework for understanding the effects of hysteron interactions on the allowed transition graphs.

C. The base graph method

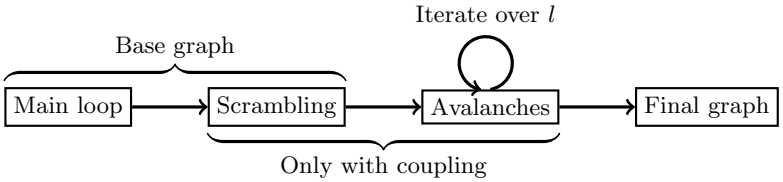

FIG. 4. Breakdown of an example transition graph into a base graph and a combination of avalanches. The base graph can itself be separated into the main loop and a number of scrambled transitions.

1. *Base graphs*

We here show how we generate the list of base graphs for N hysterons, which is subsequently used to construct the full list of candidate graphs. We first explain how base graphs can be divided up into Preisach and scrambled graphs. We then detail how one can count the num-

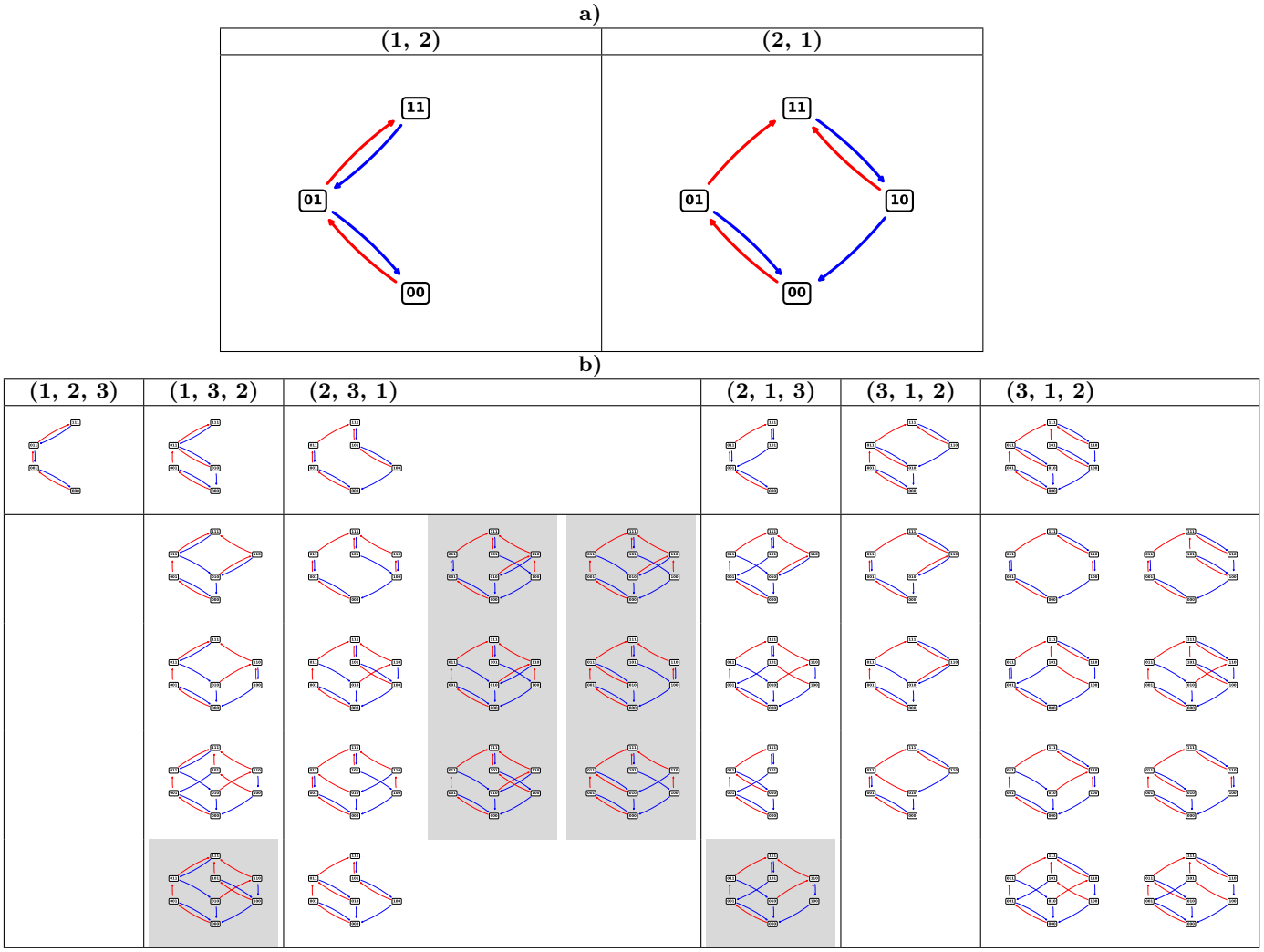

TABLE I. All possible base graphs for the two- and three-hysteron systems, indexed per main loop. a) All base graphs for $N = 2$; since scrambling is not possible for $N = 2$, the base graphs are the two Preisach graphs. b) All Preisach (top) and scrambled (bottom) base graphs for $N = 3$. Graphs on a gray background are possible for general, but not linear coupling.

ber of base graphs per main loop.

We can distinguish between two groups of base graphs. First, there are the Preisach graphs, which are possible without coupling. Second, there is a group of scrambled graphs, which are possible for interacting hysterons. Scrambling is a phenomenon previously seen in interacting hysterons[9][4], where the order in which hysterons flip is not the same throughout the graph. It occurs when the ordering between the switching fields of two hysterons in the same phase are changed by one or more hysterons, and is therefore only possible for three or more hysterons. Remarkably, having introduced the concept of base graphs, we can identify scrambling as a feature of the base graph. We can thus separate the two coupling effects of scrambling and avalanches.

In order to discuss scrambling more explicitly, we here define the main loop as the series of up and down transitions connecting the two saturated states. In the Preisach model, the ordering of the main loop fixes the transitions throughout the transition graph, so that each main loop corresponds to a unique Preisach graph. We additionally define the up and down boundary of the main loop as the series of up (down) transitions going from the state with all $s_i = 0$ (1) to that with all $s_i = 1$ (0). The number of main loops is then the number of permutations of the up boundary times that of the down boundary. Because both the up and down boundary consist of N flips, there are $N!^2$ main loops. However, we fix the up boundary when accounting for exchange symmetry, thus dividing the number of main loops by $N!$. Therefore, when accounting for exchange symmetry, there are only $N!$ main loops and resulting Preisach graphs.

In a scrambled graph, one or more of the transitions in the graph deviates from the main loop, so that each main loop corresponds to a number of base graphs (Table.I). We now explicitly calculate the number of base graphs per main loop. To start with, we observe that the number of possible up and down flips for a state S depends on

the number of hysterons that is in phase 0 or 1. Defining the magnetisation of a state as

$$M(S) = \sum_i s_i \tag{3}$$

we can state that the number of possible up flips for a state S is equal to $N - M(S)$, while the number of possible down flips is $M(S)$.
Next, we ask how many states exist with the magnetisation M. The number of states with the magnetisation M is the number of possible binary numbers that has M ones and $N - M$ zeros, which is equal to the binomial coefficient $\binom{N}{M}$.
It follows that the number of base graphs for a given number of hysterons N is

$$\#graphs = \left(\prod_{M=0}^{N} M^{\binom{N}{M}} \right)^2 \tag{4}$$

When the up boundary of the main loop is fixed to account for exchange symmetry, the number of base graphs is reduced by a factor $N!$. When the down boundary is also fixed so that the main loop is fixed, the number of base graphs is reduced by another factor $N!$. Thus, one obtains the number of base graphs per main loop:

$$\#graphs/ML = \frac{\left(\prod_{M=0}^{N} M^{\binom{N}{M}}\right)^2}{N!^2} = \left(\prod_{M=1}^{N-1} M^{\binom{N}{M}-1} \right)^2 \tag{5}$$

The number of graphs given by Equation 5 takes into account exchange symmetry, but not garden-of-Eden states (Section III A). When garden-of-Eden states are excluded, the number of base graphs turns out lower than that given in equation 5. For example, for $N = 3$, the number of base graphs provided by Equation 5 is 96, while excluding garden-of-Eden states reduces the number of base graphs to 35 (Fig. I).

2. *Avalanches*

We here show how the possible avalanches are evaluated for a given base graph.We first describe how one systematically constructs the possible avalanches of length $l = 2$ for a base graph. We then generalize our method to find graphs containing avalanches of any length l.
To help our notation, we define L as the length of the longest avalanche in a graph. For example, $L = 2$ denotes a graph that contains at least one avalanche of length $l = 2$, and no $l = 3$ avalanches. In particular, $L = 1$ denotes a base graph.
Let a base graph contain the up transition $S^{(0)} \uparrow S^{(1)}$. From the state $S^{(1)}$ there are two possible transitions: an up transition $S^{(1)} \uparrow S^{(2+)}$, and a down transition $S^{(1)} \downarrow S^{2-}$. The transition $S^{(0)} \uparrow S^{(1)}$ can thus be extended to a $l = 2$ avalanche in two ways: either by the ferromagnetic avalanche $S^{(0)} \uparrow S^{(1)} \uparrow S^{(2+)}$, or by the antiferromagnetic avalanche $S^{(0)} \uparrow S^{(1)} \downarrow S^{(2-)}$ (Fig. 5a). Similarly, a down transition $S^{(0)} \downarrow S^{(1)}$ can be extended to the antiferromagnetic avalanche $S^{(0)} \downarrow S^{(1)} \uparrow S^{(2+)}$, or to the ferromagnetic avalanche $S^{(0)} \downarrow S^{(1)} \downarrow S^{(2-)}$ (Fig. 5b). Therefore, for each transition $S^{(0)} \rightarrow S^{(1)}$, there is one possible ferromagnetic and one antiferromagnetic avalanche when $S^{(1)}$ is not a saturated state. In the case where $S^{(1)}$ is saturated, only the antiferromagnetic option exists. We must check for each of these transitions that $S^{(2)} \neq S^{(0)}$, because an avalanche cannot contain any cycles. We thus obtain a list of avalanches for each base graph, from which we construct a list of candidate graphs by evaluating each combination of avalanches.
An example for one of the $N = 2$ base graphs is shown in Fig. 6. For the example shown, the base graph has four possible $l = 2$ avalanches all associated with a different transition ($00 \uparrow 01 \uparrow 11$, $01 \uparrow 11 \downarrow 10$, $11 \downarrow 10 \downarrow 00$, and $10 \downarrow 00 \uparrow 01$), and therefore $2^4 = 16$ candidate graphs.

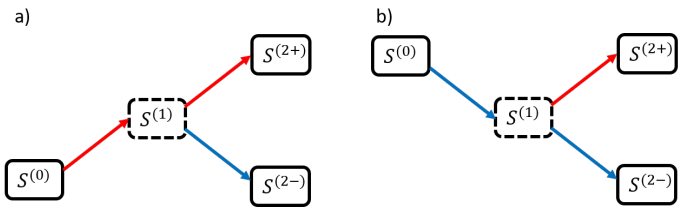

FIG. 5. Construction of an $l = 2$ avalanche by combining an incoming transition with one of at most two outgoing transitions. a) Combination of an incoming up transition with an outgoing up transition (ferromagnetic) or down transition (antiferromagnetic). b) Combination of an incoming down transition with an outgoing up transition (antiferromagnetic) or down transition (ferromagnetic)

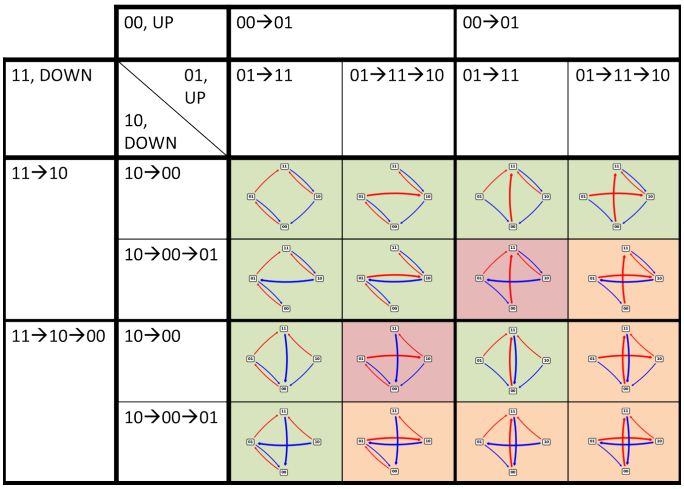

FIG. 6. All combinations of $l = 2$ avalanches for one of the two base graphs for $N = 2$ (top-left) graph, with indication of graphs that of which the design inequalities are solvable (green), solvable except for the final set of relaxation inequalities (orange) and unsolvable (red).

Thus far, we have only considered $L = 2$ graphs. We now describe how we construct graphs that have avalanches of length $L = 3$ based on the $L = 2$ graphs.

Suppose that we have a $L = 2$ graph. Similarly to how we can find $l = 2$ avalanches for a base graphs by evaluating combinations of incoming and outgoing transitions, we can construct possible $l = 3$ avalanches by finding all combinations of $l = 2$ avalanches and outgoing $l = 1$ transitions for the given graph. From the possible $l = 3$ avalanches, we can again construct a list of candidate graphs.

We now ask which $L = 2$ graphs should be used as our new 'base' for the $L = 3$ graphs. It is insufficient to use only the $L = 2$ graphs that are themselves realizable, as it is not guaranteed that a derived $L = 3$ graph will also be impossible.

We observe that, when extending a $l = 2$ avalanche to a $l = 3$ avalanche, most of the conditions required for the $l = 2$ avalanche are still included in the conditions for the $l = 3$ avalanche (see SI). The only exception is the final set of relaxation inequalities that describes the stability of the state $S^{(2)}$, which is stable for the $l = 2$ transition but unstable for the $l = 3$ transition. As a result, we can predict that for a $L = 2$ graph of which the base inequalities and the first set of relaxation inequalities are incompatible, any derived graphs with longer avalanches must also be impossible. If, however, it is only the last set of relaxation inequalities that causes the graph to be impossible, then a derived graph of $L = 3$ or higher may still be realizable.

We can thus distinguish three groups of $L = 2$ graphs, as indicated in Fig. 6. The first group of graphs is realizable, and can therefore also be used as a base to construct $L = 3$ graphs. For the second group, the graphs themselves are not realizable, but derived $L = 3$ graphs may be realizable. For the third group, neither the $L = 2$ graphs themselves nor any derived graphs containing longer avalanches are realizable. To construct all possible $L = 3$ graphs, we only need to use graphs from the first two groups.

We now generalize our method. To find all $L = l$ graphs, we construct the graphs for $L = l - 1$, and divide the graphs into the three groups as described. We then construct all $L = l$ candidate graphs for each of the $l = l-1$ graphs in the first two groups. We thus have an algorithm that constructs all realizable graphs by iterating over the maximum avalanche length L. Our algorithm terminates when none of the graphs belonging to the first and second groups have any possible avalanches of length l.

IV. APPLICATION TO SPECIFIC MODELS

We now illustrate how the base graph method is applied to the specific model where the coupling between hysterons is linear. Linear coupling entails that the switching fields $U_i^{+,-}(S)$ depend on the state S as:

$$U_i^{+,-}(S) = u_i^{+,-} - \sum_{i \neq j} c_{ij} s_j \tag{6}$$

Depending on the system, the allowed coupling coefficients c_{ij} may be restricted. We consider two instances of the linear model for $N = 3$. First, we look at the case where only one of the coupling coefficients c_{ij} is unequal to zero. Second, we look at a model for hysterons in series, where the coupling is $c_{ij} = c_j$ with all $c_j < 0$.

A. Linear coupling

B. Hysterons in series

V. DISCUSSION

VI. OUTLOOK

[1] C. W. Lindeman and S. R. Nagel, Science Advances **7** (2021).
[2] J. D. Paulsen and N. C. Keim, Science Advances **7** (2021).
[3] D. Shohat, D. Hexner, and Y. Lahini (2021), 2109.05212.
[4] H. Bense and M. van Hecke, PNAS **118** (2021).
[5] T. Jules, A. Reid, K. E. Daniels, M. Mungan, and F. Lechenault, Phys. Rev. Research **4** (2022).
[6] J. D. Paulsen and N. C. Keim, Proc. Roy. Soc. A **475** (2019).
[7] F. Preisach, Zeitschrift für Physik **94**, 277 (1935).
[8] M. Mungan, S. Sastry, K. Dahmen, and I. Regev, Phys. Rev. Lett. **123** (2019).
[9] M. van Hecke, Phys. Rev. E **104** (2021).